Available online at www.sciencedirect.com

ScienceDirect

Ceramics International 39 (2013) 8709–8714

CERAMICS INTERNATIONAL

www.elsevier.com/locate/ceramint

Sol–gel derived PMN–PT thick films for high frequency ultrasound linear array applications

B.P. Zhu[a], D.W. Wu[b], Y. Zhang[a], J. Ou-Yang[a,*], S. Chen[a], X.F. Yang[a]

[a]School of Optical and Electronic Information, Huazhong University of Science and Technology, Wuhan 430074, China
[b]CallaghanInnovation, Wellington 5040, New Zealand

Received 4 March 2013; received in revised form 10 April 2013; accepted 11 April 2013
Available online 22 April 2013

Abstract

A 12-μm PMN–PT [$0.65Pb(Mg_{1/3}Nb_{2/3})O_3$–$0.35PbTiO_3$] thick film was produced by alternate spin-coating of a ceramic powder/sol–gel composite and infiltration of the sol–gel. Using this technique, a high quality PMN–PT thick film was obtained, showing a permittivity ε_r of ~3300 and dielectric loss factor of ~0.02 at 1 kHz. Photolithographic and wet etching techniques were used to fabricate a 32-element linear array from the film. The completed array showed a center frequency of approximately 110 MHz and a bandwidth of 60% at −6 dB without a matching layer. The performance of the kerfless array was studied and compared to a kerfed array simulated with finite element analysis.

Keywords: PMN–PT thick film; High frequency; Kerfless linear array

1. Introduction

The development of high-frequency ultrasound arrays promises to improve image quality [1]. Higher ultrasound frequencies can resolve smaller features and produce finer images. Ultrasonic arrays operating over 100 MHz have the potential to provide a detailed delineation of skin anatomy for early diagnosis of cancers such as melanoma or to image useful details of small structures in other parts of the body. Despite many efforts over the past decade to develop such linear arrays [2–9], it is still not routine to achieve operating frequencies above 30 MH and the fabrication of linear arrays above 100 MHz pose even greater challenges. The main difficulty lies in the preparation of a high quality piezoelectric layer with a thickness on the order of only a few micrometers. Conventional lapping of bulk piezoelectric ceramics or single crystals is not suitable anymore as the thinned piezoelectric ceramics becomes brittle at high frequencies due to their large grain size [10]. In addition, as the operational frequency of array increases, the size of the array element will decrease. This has two implications: first, it would be difficult to form ultrasonic array elements using traditional mechanical cutting techniques; and second, a piezoelectric layer with high dielectric constant is preferred for the electrical impedance matching of array element to the electronic system.

Recent works have demonstrated that piezoelectric films of the appropriate thickness hold advantage over thinned bulk ceramics for the fabrication of ultrasound transducers with the center frequency higher than 100 MHz [11–15]. Both ZnO and PZT thick films have been proposed for high frequency (> 100 MHz) ultrasound linear array applications [6,7]. Recently, lead magnesium niobium titanate (PMN–PT) thick films with the composition near the morphtropic phase boundary (MPB) have been widely investigated. Such films are reported to possess a higher piezoelectric constant and a more desirable dielectric constant in comparison to ZnO and PZT thick films [16–20], which makes it be a promising new candidate for high frequency ultrasound technology [21]. In our previous work, PMN–PT thick film has been successfully used to build a single element transducer with center frequency above 100 MHz [22]. Hence, it is of great interest to investigate the high frequency (> 100 MHz) linear array based on PMN–PT thick film.

In this paper, the PMN–PT thick film with the thickness of 12 μm is fabricated and characterized, and a method is presented to develop a high frequency linear array from this type of film.

*Corresponding author.
E-mail addresses: oyj1106@gmail.com, goisgood@gmail.com (J. Ou-Yang).

0272-8842/$ - see front matter © 2013 Elsevier Ltd and Techna Group S.r.l. All rights reserved.
http://dx.doi.org/10.1016/j.ceramint.2013.04.054

2. Experimental process

PMN–PT thick film was made by a multi-layer spin-coating technique. A composite solution, which is the mixture of the PMN–PT powder and PMN–PT sol–gel, was spin-coated onto a 4-in. ⟨100⟩ 500-μm thick silicon wafer (Nova Electronic Materials, Ltd., Carrollton, TX). To prevent diffusion of Pb across the interface, the wafer was coated with 5000 Å thermal oxide, 200 Å Ti and 1000 Å Pt. Each spin-coating was followed by vacuum-infiltration of pure PMN–PT sol–gel in order to decrease porosity of the film. The film fabrication process was outlined in Fig. 1, Finally, a crack-free, 12-μm thick PMN–PT film was obtained.

To quantitatively characterize the properties of the film, circular Cr/Au electrodes with a diameter of 1.5 mm were sputtered as top electrodes onto the films. Dielectric properties were measured using a 4294A impedance analyzer (Agilent Technologies, Inc., Santa Clara, CA)and polarization-field (*P–E*) hysteresis properties were evaluated using a precision materials analyzer (Radiant Technologies, Inc., Albuquerque, NM). To measure the mass of the film, the film was removed from the silicon substrate, and was measured using a precision electronic balance (OHAUS Corp., Pine Brook, NJ) after clearing $Pt/Ti/SiO_2$ debris and drying.

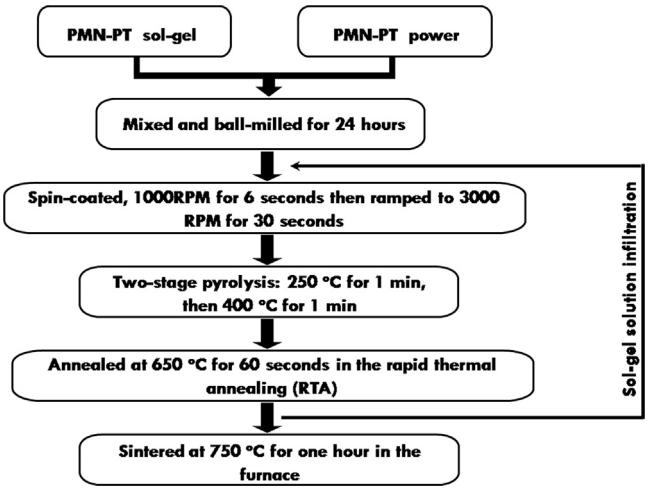

Fig. 1. PMN–PT thick film fabrication procedure.

Photolithographic and wet etching techniques were used to fabricated the PMN–PT thick film linear array. The silicon substrate is a thin, rigid and low loss solid and to avoid acoustic reverberation in this substrate, the PMN–PT film has to be transferred from the silicon to a thick absorbing substrate, such as E-solder 3022(VonRoll Isola, New Haven, CT). To transfer the film, an Au/Cr (1000 Å/500 Å) layer was first sputtered onto the film surface, followed by casting of the E-solder 3022 onto the film. The E-solder was then centrifuged and cured. The finished structure of E-solder/PMN–PT film/Si substrate was cut into 4 mm × 2 mm parts by a dicing saw and was immersed in a KOH 20% solution at a temperature of 80 °C. In a minute, the film peeled off from the silicon substrate and firmly bonded to the E-solder. The conductive E-solder substrate acts as the absorbing backing, and provides the ground electrode connection as well. From our previous experience, there is no obvious damage to the film during the transfer procedure. Afterward, Epotek-301 epoxy (Epoxy Technologies, Inc., Billerica, MA) was casted around the sample, forming non-conductive array housing. To obtain ultrasonic signals, poling treatments are required in PMN–PT thick films. The poling conditions of PMN–PT film are different from the bulk PMN–PT. A set of experiments were performed to find the optimal poling conditions for the thick film. A Cr/Au layer was sputtered onto the film surface as the top electrode and the samples were immersed in a silicon oil bath. By varying the poling temperature, poling electric field and poling time, we found out that for the PMN–PT films, the optimal values were 120 °C, 100 V and 5 min, respectively.

To measure pulse-echo response, a piece of quartz was immersed as the target in a water bath at the natural focal distance of the array. Panametrics 5900PR (Panametrics Inc., Waltham, MA) and Tektronix AFG2020 (Tektronix, Inc., Richardson, TX) function generators were used as the signal sources. The echo

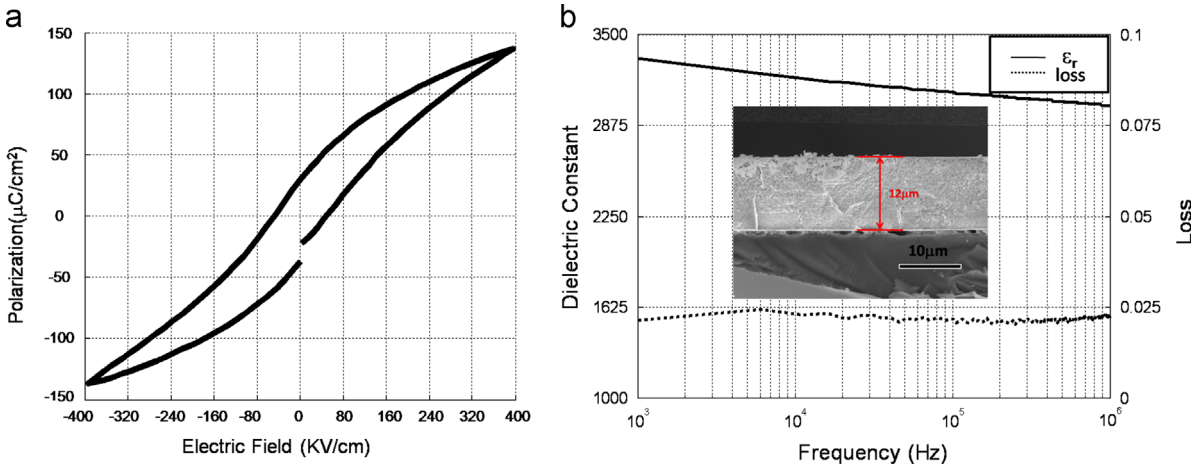

Fig. 2. Ferroelectric (a) and dielectric (b) properties of the 12-μm PMN–PT thick film. The inset: the SEM cross-sectional micrograph of the film.

signals were acquired and displayed using a LeCroy LC534 1 GHz digital oscilloscope.

3. Results and discussion

Fig. 2 shows the measured ferroelectric hysteresis loop (a) and dielectric curve (b) of the film. As can be seen, the film exhibits excellent ferroelectric and dielectric properties with remnant polarization of 29.54 μC/cm^2, the dielectric loss tangent of 0.021 and dielectric constant of 3336 at 1 kHz. Thickness of the film was measured from the SEM image as shown in Fig. 2(b). We assume the film thickness is uniform, thus volume of the film can be obtained. The density of the film was calculated to be 7000 kg/m^3, which is about 87% of bulk PMN–PT material (8000 kg/m^3). The longitudinal sound velocity of the film, estimated from the operating frequency and the thickness of the film, is around 2640 m/s. Therefore, the value of acoustic impedance ($Z=\rho c$) could be deduced to be 18.5 MRayl much lower than that of bulk PMN–PT material ($>$ 30 MRayl).

A mask was designed for patterning the 32-element linear array. In this preliminary design, the array has a kerf of 12 μm, an element width of 24 μm and an element length of 4 mm as shown in Fig. 3(a). With the mask, kerfless array elements were formed by the photolithography method. Fig. 3(b) and (c) shows the top and bottom view of the array sample after element patterning. Finally, micro-coaxial cables (Cooner Wire Company, CA) were used for electrode interconnection. To avoid the electromagnetic interference (EMI), the array was packaged in a brass tube. The connecting and packaging process is briefly illustrated in Fig. 3(d)–(j).The measured pulse-echo response and corresponding spectra of several elements, as can be seen in Fig. 4, show that performance of these array elements are very uniform, with all of the measured elements having a center frequency of 110 MHz and a −6 dB bandwidth of around 60%.

It is difficult and costly to build an electronic imaging system operating above 100 MHz to evaluate the array. Instead we used finite element simulation software PZFlex (Weidlinger Associates, Inc., Mountain View, CA) to study the beam pattern and transmitted pulses of the array. Measured properties of the film in last section were used in the simulation. To make an array in kerfless form largely decreases fabrication complexity, but it will be of great interest to compare its performance to an ideal kerfed array, where elements were mechanically isolated from each other. The kerfed array has the same modeling parameters as the kerfless array except that its kerfs are replaced with the air gap.

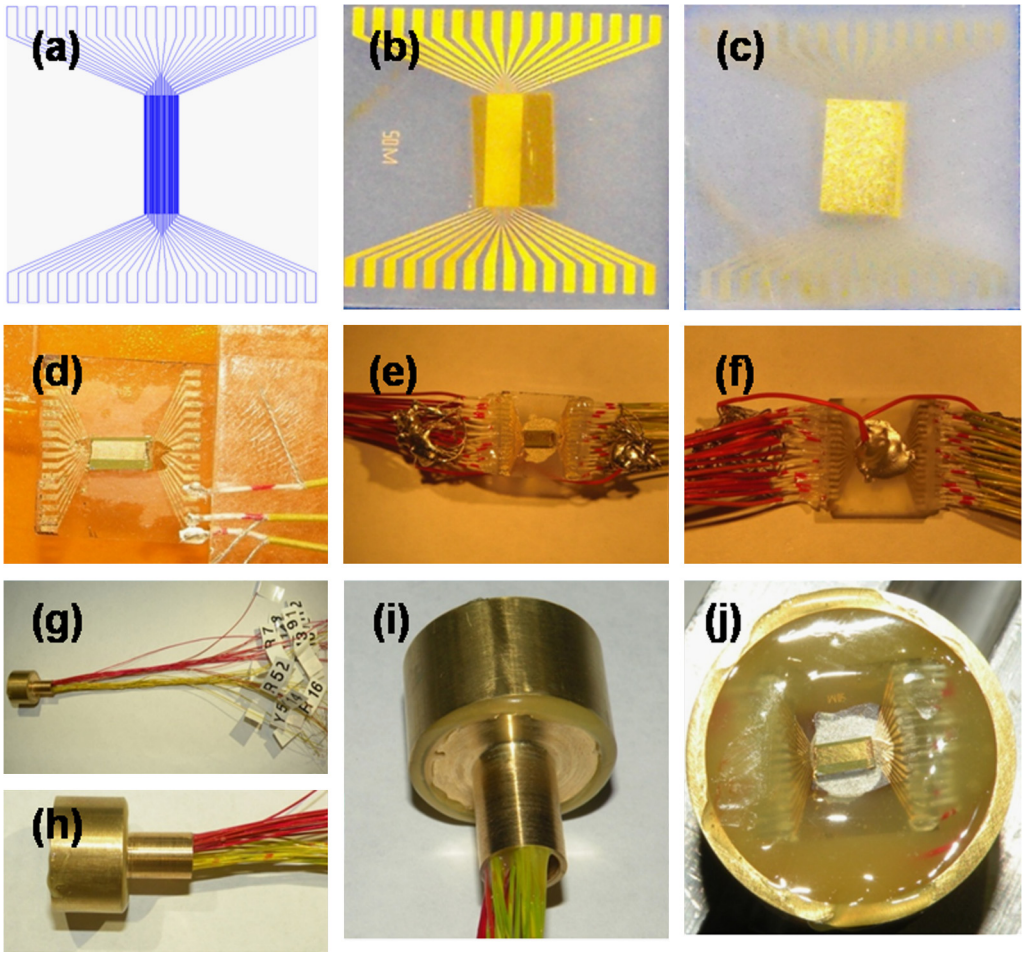

Fig. 3. Picture of the 32-element array pattern (a), top view (b) and bottom view (c) of the kerfless array before innterconneciton; connecting and packaging process (d)–(j).

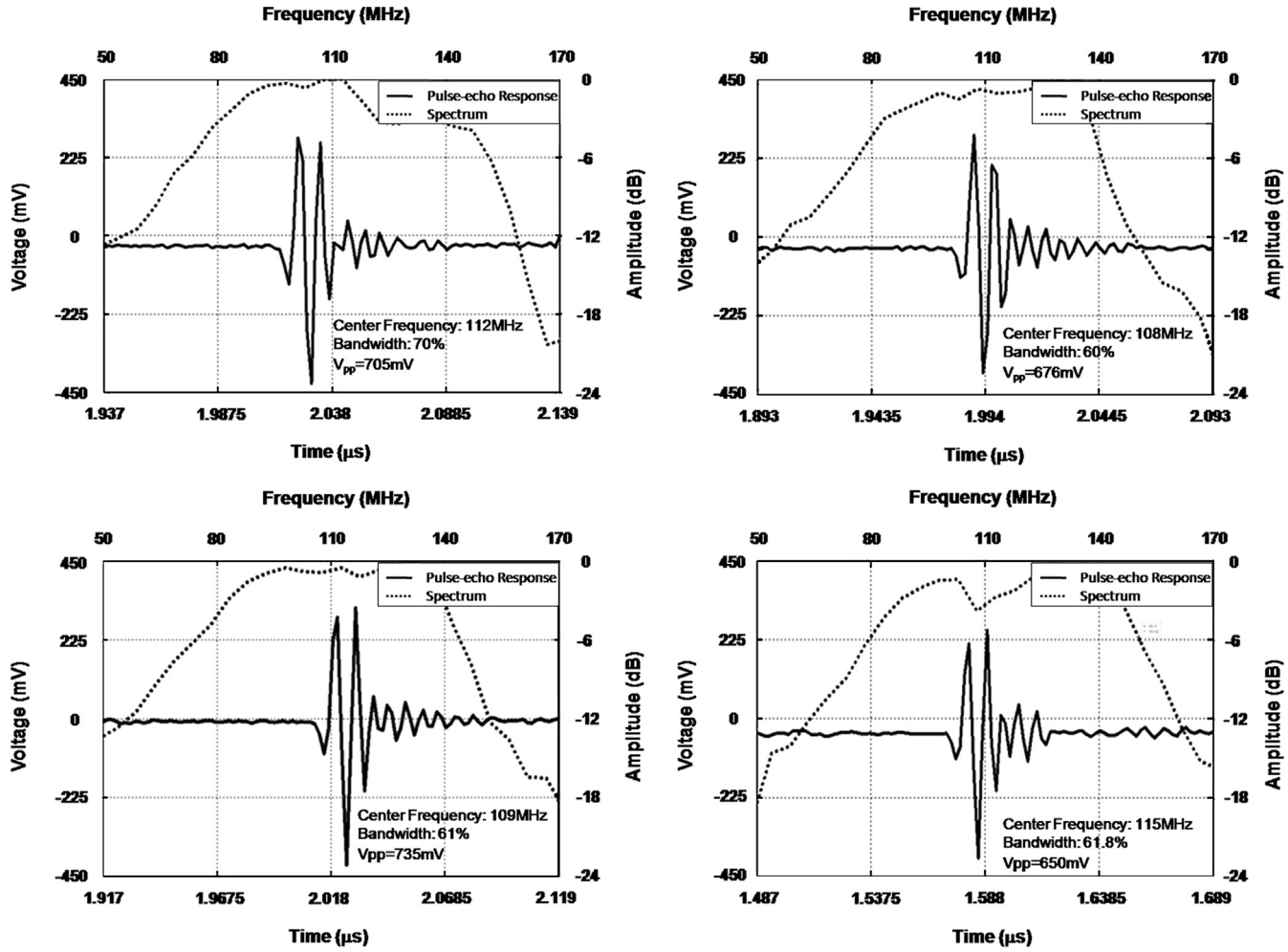

Fig. 4. Measured pulse-echo signals of PMN–PT thick film array elements.

The active aperture, which is composed of eight successive elements, was used to stuy the beam pattern of the arrays. The beam S is the summation of the eight individual elements response that contain focus dealays, which is stated as follow:

$$S = \sum_{i=1:8} W_i r(t-\tau_i) \quad (1)$$

where $\tau_i = L_i/c$, L_i is the distance between the element and the focal point and c is the acoustic velocity in the propagation medium (water); the excitation pulse $r(t)$ is the one cycle of a sine wave; a cosine window function W_i is used to suppress the side lobes. Fig. 5 shows the simulated acoustic pressure patternns of the kerfed (a) and kerfless (b) array. The plots were displayed to the same color scale. It is obvious that the kerfless one produce higer acoustic pressure than the kerfed one. That is because the kerfless array has a larger effective aperture. If we plot the acoustic pressure along the center of the beam, as can be seen in Fig. 5(c), the acoustic pressure of the kerfless array is about twice of the kerfed array in the far field, and even larger in the near field.

As shown in Fig. 5, the kerfless and kerfed arrays have quite different beam patterns at the near field, especially when the pressure is close to the array surface. In the case of the kerfed array, as shown in Fig. 6(a), the acoustic energy projects individully from corresponding elements. The magnitude differences is due to the cosine window weighing. The output of the kerfless array shown in Fig. 6(b), however, is similar to the near field beam pattern of a single element transducer. It is of great interest to study the far field of the beams. As discussed, the acoustic pressure of the kerfless array is about twice of the kered array in the far field, which indicates that the kerfless array has the potenial to provide higer sensitivity than kerfed array. If we plot the beam width laterally across the focal point (0.9 mm, in the far field), the lateral reslution of the beams can be estimated. The lateral resolution of the kerfless and kerfed beam is very close, as can be seen in Fig. 6(c) as at −6 dB, kerfed array has a lateral resolution of 50 μm and kerfless array has the lateral resolution of 56 μm. The lateral resolution of the kerfless array is slightly degraded due to the fact that the kerfless array has a larger cross-talk which increases its effective beam width.

We also studied the transmitted pulses from the active aperture to estimate the axial resolution of the arrays. The pulses were sampled at the focal point (0.9 mm, in the far field). The two arrays both show center frequencies of ~100 MHz and one-way bandwidth of ~70%. Thus, the axial resolution of the arrays is around 12 μm in soft tissues.

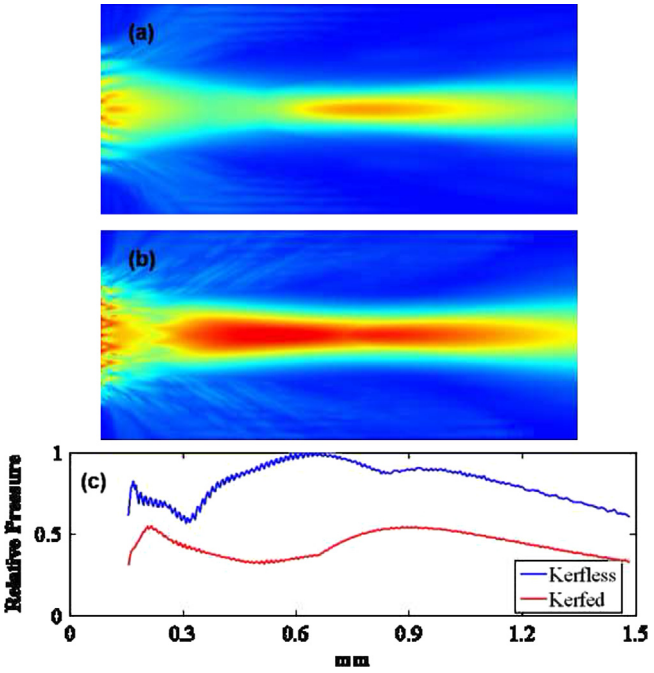

Fig. 5. Kerfered (a) array and kerfless (b) array pressure field; maxium pressure along the central line.

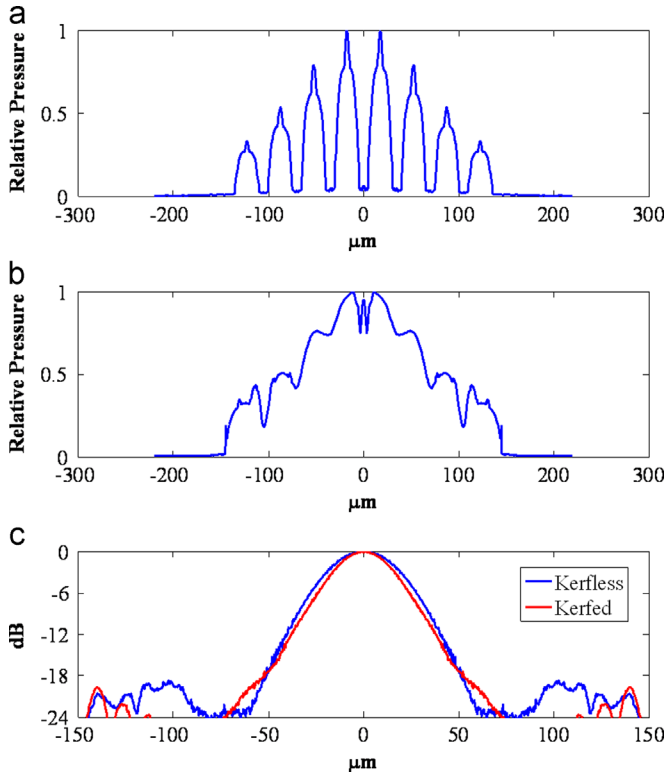

Fig. 6. Near field maxium pressure across transducer front of kered (a) and kerfless array (b); (c) the lateral beam pattern across the focus point.

As can be seen in the Fig. 7, the kerfless array has a cleaner transmitting pulse than kerfed array. This is probably because that there is no lateral mode in the kerfless array. In Fig. 7(b),

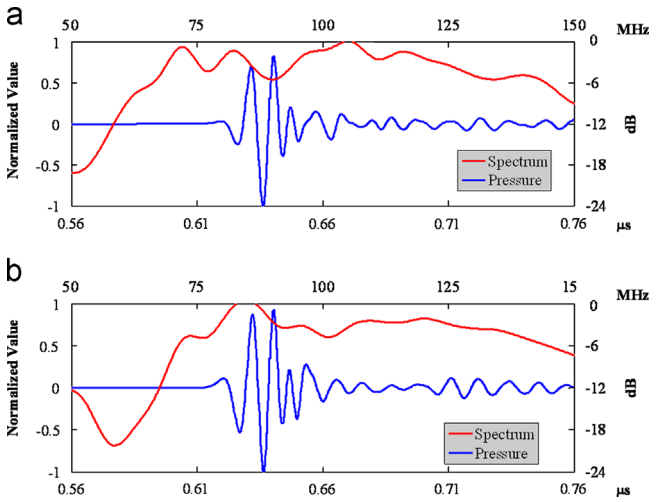

Fig. 7. Transmitted pulse at the focal point of kerfless (a) and kerfed array (b).

there is a tailling signal between 0.71 and 0.76 μs, which is the outcome of the lateral mode effect in the kerfed array elements.

4. Conclusion

High quality PMN–PT thick film was prepared with spin-coating and vacuum-infiltration techniques. The films properties that are highly desirable for ultrasound array application such as a high dielectric constant, low loss and low acoustic impedance. A method based on wet eching and photolithography, was presented to fabricate a high frequency 32-element kerfless linear array based from the film. The array was found to have a center fequency of ~110 MHz and −6 dB bandwidth of 60% without matching layer. Althrough the array is in kerfless form, which dramatically simplifies the fabrication, it shows competitive performance compared to a kerfed array: a slightly worse lateral resolution, but higher energy output, and most importantly, there is no lateral mode. The work suggests that it is feasible to fabricate linear arrays with operational freqeuncies greater than 100 MHz using PMN–PT thick films.

Acknowledgment

This work was supported by National Natural Science Foundation of China (Grant no. 51002055) and National Key Technology R&D Program in the 12th Five year Plan of China (Grant no. 2012BAI13B02). The authors would like to thank Dr Xiang Li for his assistance with the transducer fabrication process.

References

[1] K.K. Shung, J.M. Cannata, Q.F. Zhou, J.W. Lee, High frequency ultrasound: a new frontier for ultrasound, Conference Proceedings—IEEE Engineering in Medicine and Biology Society (2009) 1953–1955.
[2] J.M. Cannata, J.A. Williams, Q.F. Zhou, T.A. Ritter, K.K. Shung, Development of a 35-MHz piezo-composite ultrasound array for medical

imaging, IEEE Transactions on Ultrasonics Ferroelectrics and Frequency Control 53 (2006) 224–236.
[3] M. Lukacs, J. Yin, G. Pang, R.C. Garcia, E. Cherin, R. Williams, J. Mehi, F.S. Foster, Performance and characterization of new micromachined high-frequency linear arrays, IEEE Transactions on Ultrasonics Ferroelectrics and Frequency Control 53 (2006) 1719–1729.
[4] J.A. Brown, F.S. Foster, A. Needles, E. Cherin, G.R. Lockwood, Fabrication and performance of a linear array based on a 1–3 composite with geometric elevation focusing, IEEE Transactions on Ultrasonics Ferroelectrics and Frequency Control 54 (2007) 1888–1894.
[5] C.G. Liu, Q.F. Zhou, F.T. Djuth, K.K. Shung, High-frequency (> 50 MHz) medical ultrasound linear arrays produced by micromachining bulk PZT materials, IEEE Transactions on Ultrasonics Ferroelectrics and Frequency Control 59 (2012) 315–318.
[6] Y. Ito, K. Kushida, K. Sugawara, H. Takeuchi, A 100 MHz ultrasonic transducer array using ZnO thin films, IEEE Transactions on Ultrasonics Ferroelectrics and Frequency Control 42 (1995) 316–324.
[7] D.W. Wu, Q.F. Zhou, X.C Geng, C.G. Liu, F. Djuth, K.K. Shung, Very high frequency (beyond 100 MHz) PZT kerfless linear arrays, IEEE Transactions on Ultrasonics Ferroelectrics and Frequency Control 56 (2009) 2304–2310.
[8] Q.F. Zhou, D.W. Wu, C.G. Liu, B.P. Zhu, F. Djuth, K.K. Shung, Micromachined high-frequency (80 MHz) PZT thick film linear arrays, IEEE Transactions on Ultrasonics Ferroelectrics and Frequency Control 57 (2010) 2213.
[9] S.T. Lau, H. Li, K.S. Wong, Q.F. Zhou, D. Zhou, Y.C. Li, H.S. Luo, K.K. Shung, J.Y. Dai, Multiple matching scheme for broadband 0.72Pb$(Mg_{1/3}Nb_{2/3})O_3$–$0.28PbTiO_3$ single crystal phased-array transducer, Journal of Applied Physics 105 (2009) 094908.
[10] M. Lukacs, M. Sayer, S. Foster, Single element high frequency (> 50 MHz) PZT sol–gel composite ultrasound transducers, IEEE Transactions on Ultrasonics Ferroelectrics and Frequency Control 47 (2000) 148–159.
[11] Q.F. Zhou, S.T. Lau, D.W. Wu, K.K. Shung, Piezoelectric films for high frequency ultrasonic transducers in biomedical applications, Progress in Materials Science 56 (2011) 139–174.
[12] B.P. Zhu, D.W. Wu, Q.F. Zhou, J. Shi, K.K. Shung, Lead zirconate titanate thick film with enhanced electrical properties for high frequency transducer applications, Applied Physics Letters 93 (2008) 102905.
[13] Q.F. Zhou, C. Sharp, J.M. Cannata, K.K. Shung, G.H. Feng, E.S. Kim, Focused high frequency ZnO MEMS ultrasonic transducers for biomedical imaging, Applied Physics Letters 90 (2007) 113502.
[14] S.T. Lau, H.F. Ji, X. Li, W. Ren, Q.F. Zhou, K.K. Shung, KNN/BNT composite lead free films for high frequency ultrasonic transducer applications, IEEE Transactions on Ultrasonics Ferroelectrics and Frequency Control 58 (2010) 249–254.
[15] S.T. Lau, X. Li, Q.F. Zhou, K.K. Shung, J. Ryu, D.-S. Park, Aerosol-deposited KNN–LSO lead-free piezoelectric thick film for high frequency transducer applications, Sensors and Actuators A: Physical 163 (2010) 266 230.
[16] M. Kosec, J. Holc, D. Kuscer, S. Drnovsek, $Pb(Mg_{1/3}Nb_{2/3})O_3$–$PbTiO_3$ thick films from mechanochemically synthesized powder, Journal of the European Ceramic Society 27 (2007) 3775–3778.
[17] H. Ursic, M. Hrovat, J. Holc, M.S. Zarnik, S. Drnovsek, S. Macek, M. Kosec, A large-displacement $65Pb(Mg_{1/3}Nb_{2/3})O_3$–$35PbTiO_3$/Pt bimorph actuator prepared by screen printing, Sensors and Actuators A: Physical 133 (2008) 699–704.
[18] J. Chen, H.Q. Fan, X.L. Chen, P.Y. Fang, C. Yang, S.J. Qiu, Fabrication of pyrochlore free PMN–PT thick films by electrophoretic deposition, Journal of Alloys and Compounds 471 (2009) L51–L53.
[19] D. Kuscer, M. Skalar, J. Holc, M. Kosec, Processing and properties of $0.65Pb(Mg_{1/3}Nb_{2/3})O_3$–$0.35PbTiO_3$ thick films, Journal of the European Ceramic Society 29 (2009) 105–113.
[20] W.S. Su, Y.F. Chen, W.Y. Shih, H.Y. Luo, W.H. Shih, Domain switching in lead magnesium niobate-lead titanate polycrystalline sheets at single grain level, Applied Physics Letters 91 (2007) 112903.
[21] X. Li, W. Wei, Y.S. Chung, W.Y. Shih, W.H. Shih, Q.F. Zhou, K.K. Shung, 80-MHz intravascular ultrasound transducer using PMN–PT free-standing film, IEEE Transactions on Ultrasonics Ferroelectrics and Frequency Control 58 (2011) 2281–2288.
[22] B.P. Zhu, J.X. Han, J. Shi, K.K. Shung, Q. Wei, Y.H. Huang, M. Kosec, Q.F. Zhou, Lift-off PMN–PT thick film for high-frequency ultrasonic biomicroscopy, Journal of the European Ceramic Society 93 (2010) 2929–2931.